J Mater Sci (2008) 43:1497–1500
DOI 10.1007/s10853-007-2386-z

LETTER

Doping effect on magnetoelectric coefficient of $Pb(Zr_{052}Ti_{0.48})O_3$–$Ni_{(1-x)}Zn_xFe_2O_4$ particulate composite

Rashed Adnan Islam · Dwight Viehland · Shashank Priya

Received: 19 November 2007 / Accepted: 4 December 2007 / Published online: 18 December 2007

Magnetoelectric [ME] particulate composites combine the magnetostrictive and the piezoelectric properties of materials [1–3], through product tensor properties [4]. Compared to in situ composites produced by unidirectional solidification of $BaTiO_3$–$CoFe_2O_4$ [5–8], sintered particulate composites are advantageous because of their cost-effectiveness, ease of fabrication, and better control of their process parameters. On the other hand, laminated magnetoelectric (ME) composites consisting of piezoelectric and magnetostrictive phases have gained attention because of their superior ME response [9–12]. The laminates are fabricated by sandwiching and bonding piezoelectric plate/disk/fibers between two layers of magnetostrictive plates/disks/foils. Sintered particulate composites have inferior properties compared to the laminated ones, only because of drawbacks of low resistivity, interface defects, interface diffusion, and mismatch of elastic compliances. To enhance the ME coefficient of sintered composite, it is necessary to optimize the composition, microstructural features (grain size, grain orientation), and sintering parameters.

The figure of merit for a ferromagnetic-ferroelectric composite is given [13] as:

$$\text{Figure of merit} = \sqrt{\mu\varepsilon}; \qquad (1)$$

where μ is the magnetic permeability and ε is the dielectric permittivity. From Eq. 1, it is quite clear that a piezoelectric phase with a high dielectric constant and a magnetic phase with a high permeability would be the proper selection. Investigations have shown that nickel-based ferrite particles are very stable in a doped-PZT matrix [14] and do not react even at high sintering temperatures of 1,250 °C. Besides Mn/Ni-based ferrites are soft compared to Co ferrite, offering higher permeabilities. The advantage of Ni-based ferrite, over Mn-ferrite, is that it has a higher electric resistivity and lower dielectric loss [15].

Doping of PZT can be done to make it a soft or a hard piezoelectric [16]. Generally, acceptor dopants (Fe, Mn, Ni, Co) in PZT ceramics result in (i) decreased dielectric constant and loss, (ii) lower elastic compliance, (iii) lower electromechanical coupling factor, and (iv) lower electromechanical losses. Whereas, donor dopants (La, Sb, Bi, W, Nb) result in (i) increased dielectric constant and loss, (ii) increased elastic compliance, (iii) increased electromechanical coupling factor, and (iv) increased electromechanical losses [17].

Doping of Ni ferrite has also been done in order to improve the resistivity, permeability, magnetization and coercive field etc. [1, 6, 15, 18]. Addition of Zn to the ferrite structure increases the resistivity, permeability, and magnetization; but reduces its Curie temperature. It has been noticed that as Zn is added to the spinel structure, it usually replaces Fe^{3+} on the tetrahedral sites whereas when Fe^{3+} is replaced, the vacant octahedral sites are occupied which are emptied by Ni^{2+} [15]: Zn^{2+} has no unpaired electrons, Ni^{2+} has one, and Fe^{3+} has five. Here, the effect of doping on the magnetoelectric properties of $Pb(Zr_{0.52}Ti_{0.48})O_3$–$Ni_{(1-x)}Zn_xFe_2O_4$ composites has been studied, in order to understand the compositional dependence of the ME coefficient.

R. A. Islam
Materials Science and Engineering, University of Texas
at Arlington, Arlington, TX 76019, USA

D. Viehland · S. Priya (✉)
Materials Science and Engineering, Virginia Tech, 304A Holden
Hall (0237), Blacksburg, VA 24061, USA
e-mail: spriya@vt.edu

Ceramic compositions with stoichiometric ratios of $Pb(Zr_{0.52}Ti_{0.48})O_3$ (PZT), $0.85[Pb(Zr_{0.52}Ti_{0.48})O_3]$–0.15 $[Pb(Zn_{1/3}Nb_{2/3})O_3$ [PZT (soft)], $Pb(Zr_{0.56}Ti_{0.44})O_3 - 0.1\ Pb[(Zn_{0.8/3}\ Ni_{0.2/3})Nb_{2/3}]O_3 + 2$ (mol%) MnO_2 [PZT (hard)], and $Ni_{(1-x)}Zn_xFe_2O_4$ [NZF] (where x varies from 0 to 0.5), were fabricated by a conventional mixed oxide route. Calcination of the PZT and NZF powders was performed at 750 °C for 2 h and 1,000 °C for 5 h, respectively. X-ray patterns were taken using Siemens Krystalloflex 810 D500 diffractometer, which confirmed that the PZT was pure perovskite and the NZF spinel. The PZT and NZF powders were then mixed together as 0.8 PZT–0.2 NZF and compacted. This was followed by pressure-less sintering in air at 1,150 °C for 2 h, resulting in consolidated ceramic composites. Samples were electroded with Ag/Pd, and poled under a dc bias of 25 kV/cm for 20 min at 120 °C. Dielectric constant measurements were performed using a HP 4284 LCR meter; magnetization versus temperature (*M*–*T*) curves obtained by a quantum design physical properties measurement system (PPMS); and the ME voltage coefficient by a lock-in amplifier method. Microstructural analysis of the sintered samples was done by a Zeiss Leo Smart SEM using polished and thermally etched samples.

We used both soft and hard PZT for the fabrication of 0.8 PZT–0.2 NZF magnetoelectric composites. Figure 1a shows that the polarization of undoped PZT, hard PZT, and soft PZT, and the value of polarization under an electric field of $E = 4$ kV/mm was 14.61, 23.54, and 31.65 $\mu C/cm^2$, respectively. As well known, soft PZTs have higher polarizations per unit field applied, resulting in enhancement in both the dielectric and the piezoelectric susceptibilities. In our samples, the piezoelectric constant (d_{33}) increased from 75 to 105 pC/N and the dielectric constant increased from 642 to 914 between undoped and soft PZTs. Corresponding elastic compliance (S_{11}) of these three compositions are 1.74×10^{-11} (soft), 1.37×10^{-11} (hard), and 1.11×10^{-11} (undoped) m^2/N, respectively. Figure 1b shows the ME voltage coefficient of a PZT (soft)–20 NZF composite $\frac{\delta E}{\delta H} = 186.5\,\mathrm{mV/cm\,Oe}$. In this figure, the values of $\frac{\delta E}{\delta H}$ can also be seen to be 154 and 128 mV/cm Oe for composites made of hard and undoped PZT, respectively.

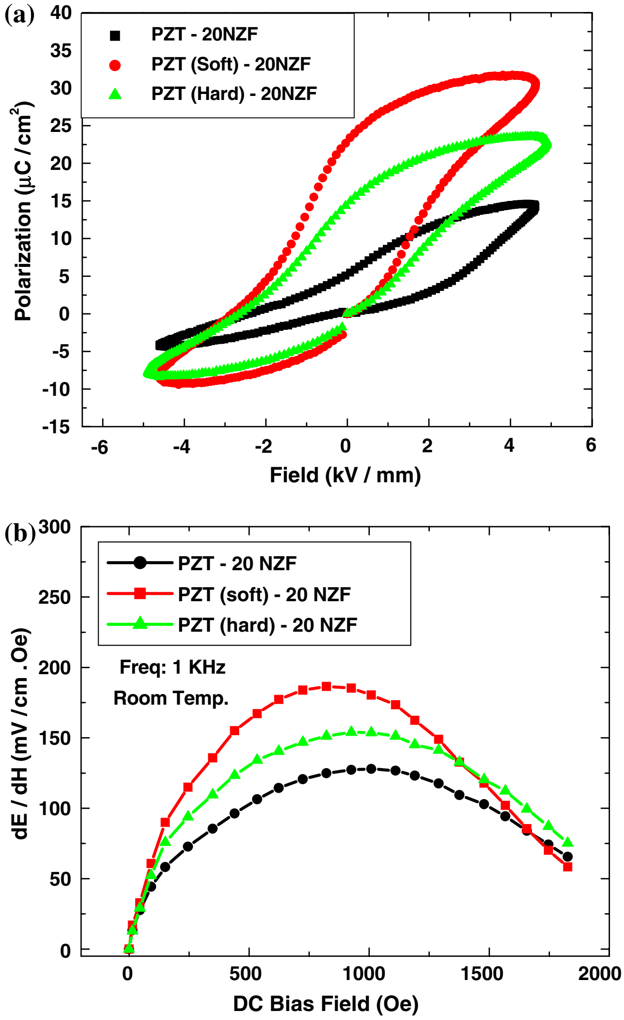

Fig. 1 (**a**) Polarization versus electric field loop and (**b**) ME coefficient versus dc bias of different compositions of PZT–20 NZF composites

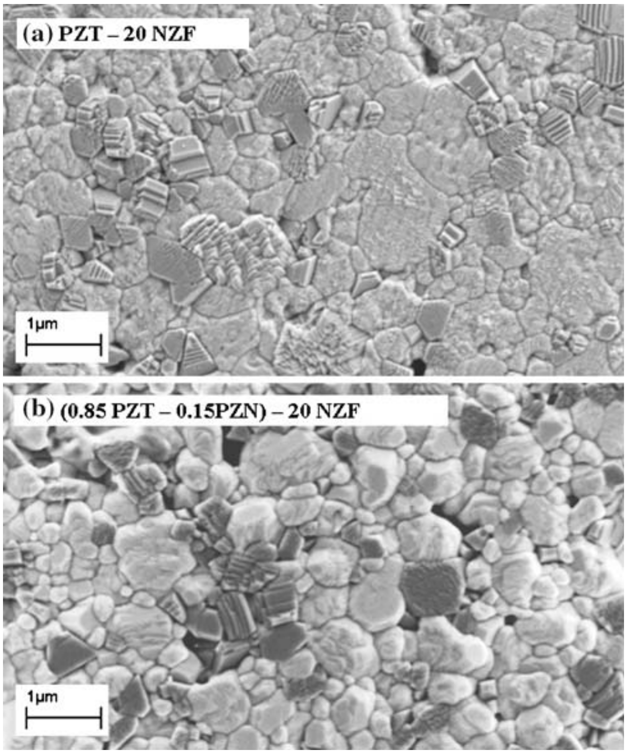

Fig. 2 Microstructure of different composites, (**a**) PZT–20 NZF and (**b**) (0.85 PZT–0.15 PZN)–20 NZF

Table 1 Piezoelectric properties of different compositions of PZT–20 NZF composite

	PZT–20 NZF	PZT (hard)–20 NZF	PZT (soft)–20 NZF
d_{33} (pC/N)	75	85	105
Dielectric constant	642	771	914
Tan δ (%)	1.26	0.82	2.7
Q_m	613	656	142

Figure 2a, b shows the microstructure of PZT (undoped)–20 NZF and PZT (soft)–20 NZF composites. Both microstructures were dense with the measured densities of ≥95%. The average grain size of the PZT–20 NZF composite was about 800–850 nm, whereas that of PZT (soft)–20 NZF was smaller and the average ranges between 650 and 700 nm. Doping of PZN in PZT reduces the grain size as both the composite were sintered at 1,150 °C for 2 h. The resistivity of PZT increases upon doping with PZN, as lower leakage currents were observed after poling of PZT (soft)–20 NZF composites (Table 1).

Figure 3a shows the saturation magnetization (M_s) and coercive field (H_c) of the PZT–20 NZF composite as a function of Zn concentration in NZF. It can be seen from this figure that with the increase of Zn concentration H_c decreases. A maximum in the magnetization (0.72 emu/g) can also be seen near 30% Zn doping, which had a coercivity of 49.6 Oe. Figure 3b shows the magnetization as a function of temperature. It can be seen that as the Zn concentration is increased the Curie temperature decreased. The Curie temperature dropped from 850 to 549 K as the Zn concentration was increased from 0 to 50 mol%.

Figure 4a shows the diffraction peak for various NZF composites ranging from pure Ni ferrite to 50 mol% Zn-doped Ni ferrite. As the Zn concentration was increased, the (400) peak shifted toward lower Bragg angles. This shift is an indication of increased values of the lattice parameters.

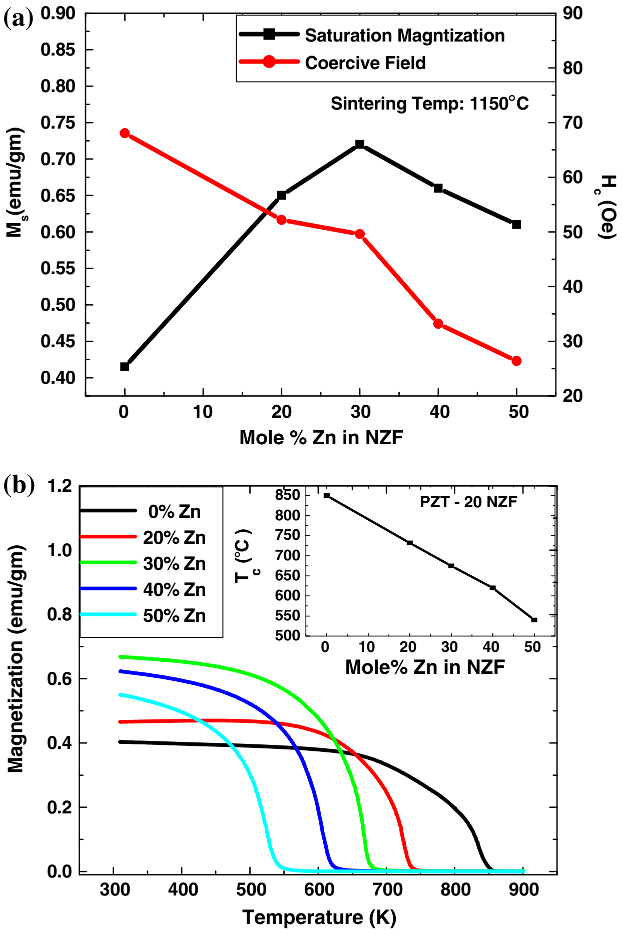

Fig. 3 Magnetic properties as a function of Zn doping. (**a**) M_s and H_c versus Zn concentration and (**b**) magnetization versus temperature

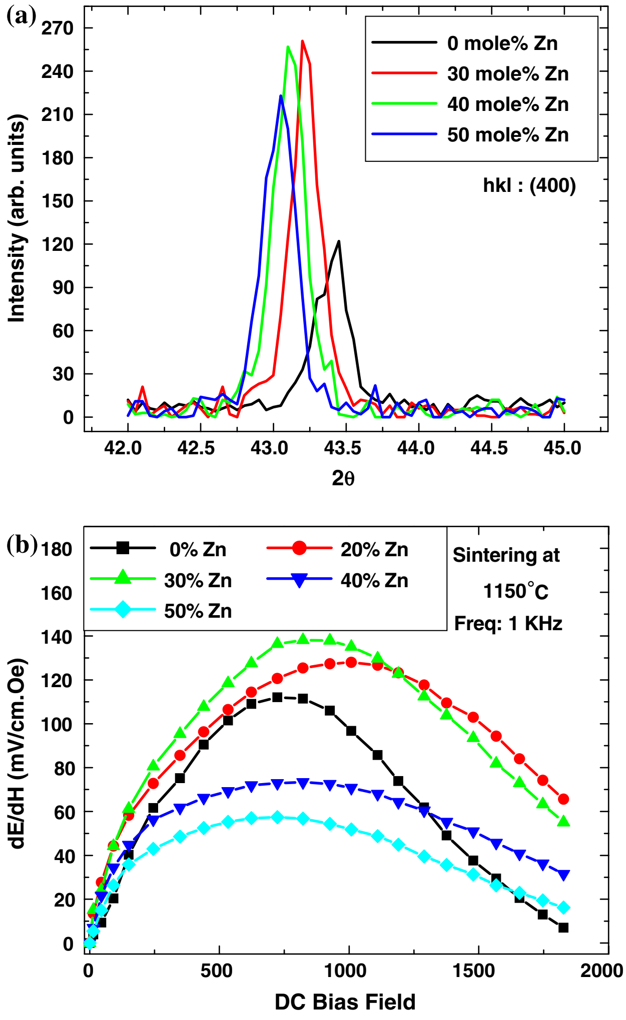

Fig. 4 Effect of Zn concentration on (**a**) peak shift of 400 peaks and (**b**) magnetoelectric coefficient of PZT–20 NZF

From Bragg's law, we determine that the lattice parameter was 8.32 Å for $NiFe_2O_4$ and 8.394 Å for $Ni_{0.5}Zn_{0.5}Fe_2O_4$: a 0.9% lattice expansion with the change in crystal chemistry. Figure 4b shows the ME voltage coefficient as a function of dc bias for different Zn concentration in PZT–20 NZF. It can be seen that as the Zn concentration was increased the ME coefficient also increased, having a maximum near 30 at.% Zn. The value of $\frac{\delta E}{\delta H}$ was 138 mV/cm Oe, whereas that of pure Ni ferrite 112 mV/cm Oe the ME coefficient was also maximum (127 mV/cm Oe) for composites with about 20 at.% Zn. With further increase in Zn concentration, the ME coefficient dropped notably, reaching a value of 60 mV/cm Oe for 50 at.% Zn. The trend of change in the ME coefficient with Zn was similar to that for the saturation magnetization. This is expected, as the permeability μ is directly related to magnetization M, via $\mu = 1 + 4\pi\frac{M}{H}$. Furthermore, the piezomagnetic coefficient is directly related to the permeability: $d_{33,\mathrm{m}} = \mu_{33}\cdot s_{33}\cdot\lambda_{33}$ [12], where s and λ are the elastic compliance and magnetostriction coefficient, respectively. Clearly the changes in the ME coefficient with Zn concentration depend on the change in effective piezomagnetic coefficient and in magnetization values.

In summary, we report a magnetoelectric composite with higher value of $\frac{\delta E}{\delta H}$, using individual phases with higher piezoelectric and higher magnetization values. We found that composites of 0.85 PZT–0.15 PZN and NZF could have ME voltage coefficient as high as 187 mV/cm Oe. This is quite a large magnitude for a (0–3) all-ceramic composite that has been cosintered.

Acknowledgement The authors are sincerely thankful to Prof. Ping Liu's research group (UTA) for their help in the magnetic characterization. This study was supported by the Army Research Office.

References

1. Ryu J, Carazo AV, Uchino K, Kim H (2001) J Electoceram 7:17
2. Flores VC, Baques DB, Flores DC, Aquino JAM (2006) J Appl Phys 99:08J503
3. Lupeiko TG, Lisnevskaya IV, Chkheidze MD, Zvyagintsev BI (1995) Inorg Mater 31:1139
4. Ryu J, Priya S, Uchino K, Kim H (2002) J Electroceram 8:107
5. Boomgaard JVD, Van Run AMJG, Suchtelen JV (1976) Ferroelectrics 10:295
6. Boomgaard JVD, Born RAJ (1978) J Mater Sci 13:1538
7. Boomgaard JVD, Terrell DR, Born RAJ, Giller HFJI (1974) J Mater Sci 9:1705
8. Van Run AMJG, Terrell DR, Scholing JH (1974) J Mater Sci 9:1710
9. Ryu J, Priya S, Uchino K, Viehland D, Kim H (2002) J Kor Ceram Soc 39:813
10. Srinivasan G, Rasmussen E, Levin B, Hayes R (2002) Phys Rev B 65:134402
11. Dong SX, Zhai J, Li JF, Viehland D (2006) J Appl Phys 88:082907
12. Dong S, Zhai J, Li JF, Viehland D (2006) Appl Phys Lett 89:252904
13. Islam RA, Priya S (2006) J Appl Ceram Tech 3(5):353
14. Kramer WE, Hopkins RH, Daniel MR (1977) J Mater Sci Lett 12(2):409
15. Newnham RE (1989) Rep Prog Phys 52:123
16. Jaffe B, Cook WR, Jaffe H (1971) Piezoelectric ceramics. Academic Press, Massachusetts, USA
17. Islam RA, Priya S (2006) J Am Ceram Soc 89(10):3147
18. Devan RS, Chogule BK (2007) J Appl Phys 101:014109